# Density-functional calculations for small iron clusters: $Fe_n$, $Fe_n^+$, and $Fe_n^-$ for $n \leq 5$

Miguel Castro* and Dennis R. Salahub
*Département de Chimie et Centre d'Excellence sur la Dynamique Moléculaire et Interfaciale, Université de Montréal, C.P. 6128, Succursale A, Montréal, Québec, Canada H3C 3J7*
(Received 8 November 1993; revised manuscript received 25 January 1994)

The optimum geometries, electronic and magnetic structures, bond dissociation energies (BDE's), binding energies ($D_e$'s), ionization potentials (IP's), and electron affinities (EA's) of small iron clusters are studied by means of a *linear combination of Gaussian-type orbitals–local and/or nonlocal spin-density* method. At the nonlocal level and with respect to nonspherical iron atoms the calculated $D_e$'s are 1.04, 1.41, 1.87, and 2.20 eV/atom for $Fe_2$, $Fe_3$, $Fe_4$, and $Fe_5$, respectively. The calculated IP's are 8.16, 7.01, 6.34, 6.20, and 6.52 eV for Fe, $Fe_2$, $Fe_3$, $Fe_4$, and $Fe_5$, respectively, in reasonable agreement with their experimental counterparts of 7.9, 6.3, 6.4–6.5, 6.3–6.5, and 5.9–6.0 eV, and also are close to those obtained by means of *ab initio* techniques. The lowest-energy states are those with a maximum number of nearest-neighbor (short) bonds, and with high magnetic moments (3, 2.67, and 3 spins per atom for $Fe_2$, $Fe_3$, and $Fe_4$; in $Fe_5$ the magnetization is unevenly distributed and ranges from 2.90 to 3.31 spins per atom) coupled ferromagnetically. The gain in magnetic energy promotes the close-packed structures (for $n=3$ and 4) or small distortions into somewhat more open geometries (for $n=5$). The importance of the *s* electrons for the bonding properties increases with increasing cluster size; starting from predominantly localized *d* bonds on earlier clusters, the chemical bond evolves to show a delocalized *s* pattern at the Fermi level for the larger clusters. The equilibrium bond lengths, for the computed ground states (2.00, 2.10, and 2.22 Å for $Fe_2$, $Fe_3$, and $Fe_4$, respectively; whereas in $Fe_5$ they range from 2.23 to 2.63 Å) are much shorter than the shortest distance in the bulk, 2.48 Å, although for the pentamer some bond lengths approach the bulk value. The fully optimized cations, $Fe_n^+$, and anions $Fe_n^-$, occur in similar structures as those of the ground states; in general, $Fe_n^+$ show a larger structural relaxation than $Fe_n^-$.

## I. INTRODUCTION

Transition-metal (TM) cluster properties of ferromagnetic elements present a challenge to state-of-the-art experimental and theoretical techniques. For example, recent beam experiments have found a complex magnetic behavior of size-selected iron and cobalt clusters,[1,2] not anticipated previously.[3] The clusters deflect toward increasing magnetic field with effective magnetic moments $\mu_{\text{eff}}$ per atom far below the bulk moments. This was identified as superparamagnetism by Khanna and Linderoth,[4] where each cluster has a large magnetic moment, equal to the ferromagnetic alignment $n\mu$ of the $n$ atomic moments of the $n$ atomic moments in the cluster. With this model and with the cluster-temperature-dependent results of Bucher, Douglas, and Bloomfield,[2] it was found that the true moment $\mu$ of small $Co_n$ clusters, of $2.08\mu_B$, is indeed enhanced (by about 20%) over the bulk value,[4] whereas for $Fe_n$ a lower bound of $2.2\mu_B$ for the true $\mu$ was established.[4] As a measure of the binding of these highly polarized valence electrons, the ionization potentials (IP's) of $Fe_n$ ($n \leq 25$), determined by Rohlfing *et al.*,[5] start to decrease nonmonotonically from the atomic IP toward the bulk work function as $n$ increases. Lastly, there has been studied[6,7] the collision-induced dissociation of $Fe_n^+$ ($n=2-19$). In this way, and using the known adiabatic IP's,[5] were determined the bond dissociation energies (BDE's) of ionic and neutral iron clusters. The trends exhibited by these size-dependent properties imply complicated electronic structures, unique and nonbulklike, in which the spin-polarization effects may play an important role[5] and indicate a nontrivial evolution from insulating (more localized electrons) to metallic behavior (more itinerant electrons).

Cluster properties may also depend sensitively on the geometry. But experimental bond lengths ($R_e$) and bond angles for TM clusters are scarce. Even for the dimers the experimental data are not yet complete and some $R_e$ values show large uncertainties.[8]

On the theoretical side, it is only very recently that modern techniques have proven their ability to determine the lowest-energy structures of relatively large clusters. In particular, *s*- and *sp*-valence-electron systems have been relatively well studied;[9–11] and trends and features of the most favored geometries of the ground electronic states have been characterized. Due to the complexity of the TM atomic forces, which arise from the complex TM-TM exchange-correlation interactions, calculations on TM clusters commonly are done with the constraints of *frozen* bond lengths and/or bond angles, usually equal to the bulk values. This kind of calculation has been widely used as models for the metal surface-ligand interactions that occur in catalytic processes.[12] For instance, using *ab initio* techniques and chosen fragments of the unit bcc cell of iron, Tatewaki, Tomonari, and Nakamura[13] have performed electronic-structure and IP calculations on $Fe_2$–$Fe_6$. Although reasonable results were obtained,[13] the calculated IP's were somewhat below the experiment values. It was pointed out[13] that further discussion of ionization potentials, in this kind of

 

system, qualitatively requires geometry optimization as well as the inclusion of correlation.

The implementation of analytical energy gradients in density-functional theory (DFT),[14–17] together with the inclusion of electron correlation via the exchange-correlation functional at the local and nonlocal levels of DFT,[17] have allowed an accurate and full optimization of bond lengths and bond angles in main group molecules and in complex TM systems.[16–22] Using the local spin-density approximation (LSDA), the calculated equilibrium bond lengths are typically within 0.02 Å or so of the experimental values and the angles are within 1°,[17–20] whereas the vibrational frequencies lie within 5% of the experimentally observed frequencies.[17,18] The use of nonlocal functionals substantially improves the atomic and molecule exchange-correlation energy results and affords estimates of TM-ligand and TM-TM binding energies which, at this level of theory, are remarkably close to the proposed experimental values.[21,22] Indeed, at this level of sophistication, the recently developed DFT techniques are powerful and useful tools for the analysis of properties and processes of systems (clusters, surfaces, metal-ligand interactions, etc.) which involve TM atoms.

Recently, Chen *et al.*,[23] using the LSDA, have determined the structural and magnetic properties of neutral $Fe_n$, $n \leq 4$. However, the LSDA substantially overestimates the BDE's and binding energies ($D_e$'s) of TM clusters.

Here we report the results of first-principles all-electron calculations, using DFT local and nonlocal exchange-correlation potentials, for neutral ($Fe_n$) and charged ($Fe_n^+$, $Fe_n^-$) iron clusters up to $n=5$. We demonstrate the power of these techniques for the analysis of the binding of electrons and atoms and of the bond strengths within the cluster (IP's, $D_e$'s, and BDE's). The computed electronic structures allow insight into the observed trends and the main features involved in the stability of these magnetic clusters. A brief report of some of the main results has already appeared.[24]

## II. COMPUTATIONAL PROCEDURE

We have used the code deMon:[17] a method based on linear combination of Gaussian-type orbitals DFT. The LSDA was included as in Ref. 25, while the nonlocal spin density (abbreviated here simply as NL, for "nonlocal") gradient-type corrections were those of Perdew and Wang (1986) for exchange,[26] and Perdew (1986) for correlation.[27] The nonlocal potential was included in the Kohn-Sham potential during the self-consistent-field (SCF) procedure. Numerical instabilities in the nonlocal functional, which arise when the ratio of the density gradient to the density becomes too large, were removed by means of a damping factor.[28]

In these cluster calculations, all electrons were treated explicitly. For each iron atom, a (43 321/43/41+) orbital basis set optimized for the bonding $3d^74s^1$ atomic configuration[29] was used. (Indeed, it will be shown below that in these $Fe_n$ clusters the Fe atom is close to $3d^74s^1$.) This basis was decontracted into (43 321/4211*/311+), in which a $p$-polarized function was taken from the (63 321/5211*/41+) basis set constructed as in Ref. 30. The auxiliary basis set, used in the fitting of the charge density (CD) and the exchange-correlation (XC) potential has the pattern (9,4;9,4). In this notation $(k_1,k_2;l_1,l_2)$, $k_1$ ($l_1$) is the number of $s$-type Gaussians in the CD (XC) basis and $k_2$ ($l_2$) is the number of $s$-, $p$-, and $d$-type Gaussians constrained to have the same exponent in the CD (XC) basis. The charge density was fitted analytically, while the XC potential was fitted numerically on a FINE grid[31] comprised of 32 radial shells and 26 angular points per shell, giving rise to a total of 832 points per atom.[32] At the end of each SCF procedure, the exchange-correlation contribution to the energy gradients were calculated by numerical integration on an augmented set of grid points consisting of the same 32 radial shells with 50, 110, or 194 angular grid points.[31]

Without imposed symmetry constraints, and by means of the Broyden-Fletcher-Goldfarb-Shanno (BFGS) algorithm,[33] the geometries were optimized by minimizing the norm of the gradient with a threshold of $10^{-4}$ a.u. All $R_e$'s and bond angles were simultaneously refined, and several candidates were tried in each case so as to locate different minima on the potential energy surface (PES). The BFGS algorithm searches the PES through its first derivatives, evaluated analytically, and through approximate second derivatives (the Hessian matrix) updated numerically. This affords an efficient method for finding the best search directions and the optimal distance to move along that search direction.

In our spin-polarized calculations, the standard Mulliken population analyses were done to obtain both the charge on each atom and the unpaired-spin population. In the course of the geometry optimization of a given cluster, several electronic configurations of different spin were tried. Though convergence difficulties were found, due to near degeneracy at the Fermi level, all these $Fe_n$ clusters were converged to integral spin-orbital occupation numbers as shown in the tables deposited in the AIP's Physics Auxiliary Publication Service. Such tables contain the Mulliken population analyses for the calculated ground states of $Fe_n$ ($n \leq 5$). See Ref. 17 for more computational details.

In order to test the basis set and the LSDA and NL functionals we have calculated the $^5D(3d^64s^2) \rightarrow {}^5F(3d^74s^1)$ excitation for the iron atom, for which the experimental result is 0.875 eV.[34] Using spherical atoms (the five $3d^\downarrow$ orbitals have equal occupation numbers, $\frac{1}{5}$ of an electron each, for $^5D$, or $\frac{2}{5}$ of an electron each, for $^5F$), the LSDA gives a $^5D$-$^5F$ separation of 0.25 eV. The inclusion of nonlocal corrections improves this value to 0.51 eV. Further, the removal of the constraint of a spherical atomic charge density[35] (nonspherical iron atoms are constructed by assigning integral occupation numbers to the $3d^\downarrow$ orbitals) in the NL SCF calculation produces a $^5D$-$^5F$ splitting equal to 0.30 eV. It should be stated that the nonspherical calculations are neither obvious to define (electrons may be assigned to the available spin orbitals in several ways and several calculations are needed to find the minimum energy) nor facile to converge. When viewed in the context of the inherent ambiguity about treating multiplets within Kohn-

Sham DFT, it seems that high accuracy for the splittings should not be expected for such complex open-shell systems as the iron atom. Below we will argue that the errors in the calculations of the binding energies for $Fe_n (n \leq 5)$ may be traced, at least partially, to the errors in the description of the iron atom. In the nonspherical calculations, $s$ and $d$ orbitals mix and so the labels $3d^6 4s^2$ and $3d^7 4s^1$ are only approximate (as is also the case in a correlated *ab initio* calculation). For the $^5D$ ($3d^6 4s^2$) state we find, via Mulliken analysis, a configuration of $3d^{6.4} 4s^{1.6}$ whereas the $^5F$ ($3d^7 4s^1$) states is calculated as $3d^{7.02} 4s^{0.98}$. The hartree-Fock SCF calculations gave a $^5D - {}^5F$ separation at least twice the experimental number, depending on basis-set size.[13,36] After the inclusion of correlation this splitting was improved to 1.32 eV.[13] Finally, the total-energy difference between neutral and ionic iron atoms is 8.08 eV (LSDS) and 8.16 eV (NL); both values are close to the experimental IP,[37] 7.90 eV.

## III. RESULTS

### A. Structures

The ground states (structures 2a, 3a, 4a, and 5a in Fig. 1) of $Fe_n$ ($n \leq 5$) are ferromagnetic, with a high number of nearest-neighbor bonds (NNB's) and with average magnetic moments $\mu$ enhanced over the bulk value of $2.2\mu_B$ by 22–45 %. The latter is in agreement with the experimental results of Bloomfield and co-workers[38] who have found, by ion-beam techniques, that the moment $\mu$ of small iron clusters is enhanced by about 27% over the bulk value. Moreover, in the biggest of our studied clusters, 5a, there is an anisotropic distribution of atomic moments ($2.8\mu_B - 3.2\mu_B$, depending on the chemical environment or number of NNB's of the Fe atom); the average value, $3.0\mu_B$, is close to that found by beam techniques,[38] $(2.8 \pm 0.2)\mu_B$. In the ground states 2a–4a the $R_e$'s are much shorter than the shortest distance in the bulk, 2.48 Å, whereas in 5a there are various short values, close to that of 4a, along with $R_e$'s close to, but larger than, 2.48 Å. Another interesting feature is that the relative energy of the isomers (see Fig. 1) with respect to the corresponding ground state decreases with increasing cluster size; which is in agreement with the experimental observations.[7]

In Fig. 1 we have also indicated the multiplicity $M(=2S+1)$, the total spin $S$, and the number of spins per atom in Bohr magnetons ($\mu_B$), for each isomer. It will be shown below that different states of a given $Fe_n$ ($n \leq 5$) cluster give rise to different types of chemical bonds, to different patterns of charge distributions, and to different magnetic arrangements (depending on the local chemical environment, as measured by the number of NNB's). This is clearly displayed by the isomers; for example, whereas in 4b short covalent bonds occur predominantly, in 4c both longer "metallic" (between the atoms separated by 2.43 Å) and shorter covalent bonds (between the atoms separated by 2.02 Å) occur. We will now discuss the main findings for each cluster.

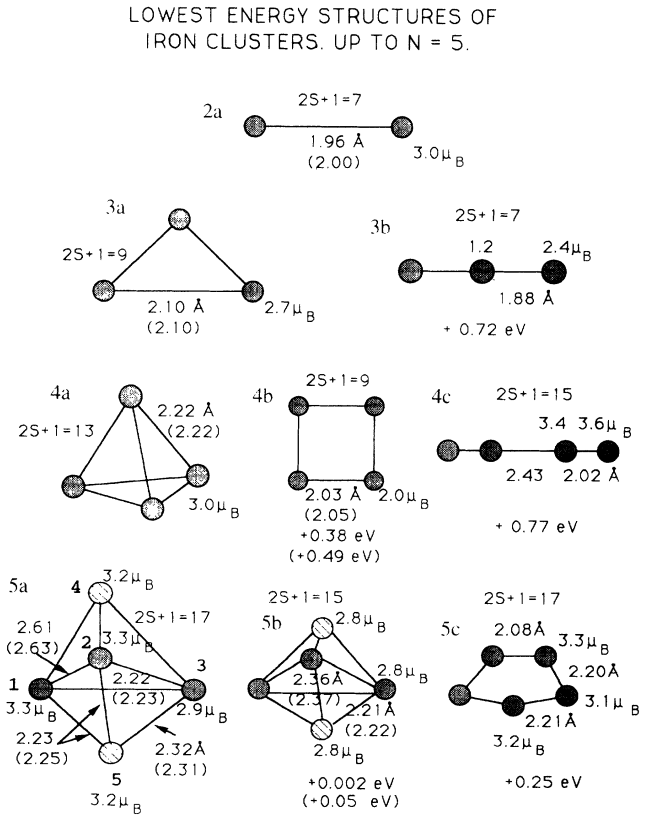


FIG. 1. Lowest-energy structures of $Fe_n$ ($n \leq 5$). Ground states are 2a, 3a, 4a, and 5a for $n = 2$, 3, 4, and 5, respectively. Also indicated are the LSDA and NL (values in parentheses) relative energies of the isomers (in eV/atom), the multiplicity $2S+1$, the spin per atom (in bohr magnetons), and the LSDA and NL (values in parentheses) equilibrium bond lengths.

### B. $Fe_2$

The LSDA $R_e$ of $Fe_2$ is 1.96 Å. The NL $R_e$, 2.00 Å, is closer to the value determined in the less polarizable neon matrix, 2.02 Å,[39] which should more closely resemble the $R_e$ of $Fe_2$, than that measured in an argon host, 1.85 Å.[40] The spin-polarized configuration for the valence molecular orbitals (MO's) of $Fe_2$ (see Table 1 in PAPS[17(c)]). $\{1\sigma 1\pi^2 1\delta^2 2\sigma 1\delta^{*2} 1\pi^{*2} 1\sigma^*\}^{\uparrow} \{1\sigma 1\pi^2 2\sigma 1\delta_{Ef}\}^{\downarrow}$, is consistent with a $^7\Delta_u$ molecular state, places the Fermi level ($E_F$) at the minority $d\delta^{\uparrow}$ weakly bonding MO, and indicates formally a double $d$ and a single (from $s\sigma^{\uparrow\downarrow}$)$s$ bond. Tomonari and Tatewaki[41] have found a large $d$ contribution to the bonding in the $^7\Delta_u$ state of $Fe_2$. These results of a multiple $d$-bond formation, in addition to the $4s\sigma$ single bond, are in disagreement with the earlier *ab initio result* of a single bond in $Fe_2$, almost entirely due to the $4s\sigma_g$ MO.[42]

The quintet state of $Fe_2$, with $R_e = 1.811$ Å (LSDA) or 1.814 Å (NL), is located 0.598 eV (0.79 eV) above the septet ground state at the LSDA (NL) level. Further occupancy of the minority-spin manifold until the $S=0$ state is reached produces a nonmagnetic state for $Fe_2$, with $R_e = 1.80$ Å (LSDA) or 1.83 Å (NL), which is located 2.32 eV (2.55 eV) above 2a, at the LSDA (NL) level. Its

instability with respect to the ferromagnetic ground state is a result of the tendency of the system to maximize the gain in magnetic energy through an enhancement of the exchange energy (which in turn maximizes the $\sigma$, $\pi$, and $\delta d$ bonding). This result agrees with that of Chen *et al.*,[23] who have found that the nonmagnetic state of $Fe_2$, with $R_e = 1.83$ Å, is located 2.32 eV (1.16 eV/atom) above the ground state. The range of the $d$ exchange splitting in this *microferromagnet,* structure 2a, $1.7(1\sigma)-2.5(1\delta)$ eV, is close to the ferromagnetic bulk, 1.6–2.7 eV, computed by means of band theory,[43] and to that of a ferromagnetic $Fe_{15}$ cluster, 1.2–3.2 eV, calculated by means of the SCF $X\alpha$ scattered-wave (SCF $X\alpha$-SW) method, with $R_e$'s = 2.48 Å.[44]

The $M=7$ state of $Fe_2$ with $R_e = 2.48$ Å (a bulk fragment) is located 1.39 eV (LSDA) or 0.94 eV (NL) above the structure 2a. It will be shown below that in going from a given bulk fragment (a cluster with $R_e$'s = 2.48 Å) to the optimized geometry for that fragment, the local potential gives a relatively large difference of total energy; the introduction of NL corrections reduces this difference dramatically.

### C. $Fe_3$

The LSDA indicates the structure 3a in Fig. 1 as the ground state for $Fe_3$, with $R_e$'s = 2.10 Å and with $S=4$. The linear combination of atomic orbitals (LCAO)[23] and the SCF-$X\alpha$-SW[5] calculations have found 3a with $R_e = 2.04$ Å,[23] and $R_e = 2.00$ Å,[5] and with $S=4$. The far-infrared spectra suggest that $Fe_3$ is bent,[45] since the symmetric stretching mode would otherwise be infrared inactive. In fact, the linear structure 3b is 2.16 eV higher (0.72 eV/atom), with $S=3$ and $R_e$, 1.875 Å, shorter than that of $Fe_2$. Similar results were reported by Chen *et al.*[23] for the structure 3b: 0.82 eV/atom higher, $S=3$, and $R_e = 1.92$ Å.

The Mulliken population analysis for the valence MO's of the computed ground state 3a (see Table II in PAPS[17(c)]) indicates a *nonet* ground state for $Fe_3$, $M=9$. Then, the chemical bond formation, a spin-pairing process, has removed 1.33 spin/atom (with respect to the limit of separated species, where each iron atom has 4.0 spins). In 3a $E_F$ is $d^{\downarrow}$ type. Another feature is the splitting of the majority-spin ($\uparrow$) MO's into lower (bonding) and upper (antibonding, labelled by * in Table 2 of PAPS[17(c)]) branches, as in $Fe_2$. It was pointed out previously[5] that the ground states of $Fe_2$ and $Fe_3$ show similar electronic structures; below, we will show that this picture remains for their cations.

In our LSDA calculations, the nonmagnetic state of $Fe_3$ in the triangular geometry is located 1.22 eV/atom above the ground state 3a, with $R_e = 2.01$ Å. Chen *et al.*[23] have found this nonmagnetic state 0.99 eV/atom above 3a, with $R_e = 1.97$ Å.

### D. $Fe_4$

The three-dimensional (3D) structure 4a was found to be the ground state for $Fe_4$, with $R_e$'s = 2.22 Å, $S=6$, and a high number of NNB's, three per atom. The 2D geometry 4b is higher in energy than 4a, by 1.94 eV for NL and by 1.5 eV for the LSDA, with shorter $R_e$'s, 2.03 Å (LSDA), a lower magnetization, $S=4$, and a lower number of NNB's, two per atom. Similarly, Chen *et al.*[23] have found 4b (with $R_e = 2.05$ Å, $S=4$) 1.12 eV above 4a (with $R_e = 2.25$ Å, $S=6$). (This is not the case for the $s$-type alkali-metal clusters where the sodium aggregates, for instance, do not always saturate the number of nearest-neighbor bonds and Jahn-Teller distortions drive the tetramer, and the pentamer, toward 2D planar geometries.[9] Even in silicon clusters the $sp$ hybridization drives the tetramer into a 2D rhombus.[10,11])

The linear geometry 4c, with $R_e$'s = 2.02 and 2.43 Å, is located 3.06 eV above 4a. 4c resembles two dimers joined by a weak "metallic" bond (2.43 Å is remarkably close to the shortest $R_e$ in the bulk, 2.48 Å) and also reaches a high spin state, $S=7$.

The Mulliken population analysis for the ground-state structure 4a indicates an $s^{\uparrow}$-like $E_F$ for $Fe_4$ (see Table III in PAPS).[17(c)] The nonmagnetic state of $Fe_4$ (in the tetrahedral geometry) is located 0.93 eV/atom (LSDA) above 4a. The $R_e$'s of this $S=0$ state have been shortened to 2.09 Å. Chen *et al.*[23] have located this state 0.79 eV/atom above 4a, with $R_e$'s = 2.12 Å.

### E. $Fe_5$

After the optimization procedure for $Fe_5$, the distorted trigonal bipyramid 5a, $S=8$, was found to be of lowest energy. This structure was reached from the $S=8$ state of a square pyramid with $R_e = 2.48$ Å, see below, through a simultaneous optimization of bond lengths and bond angles; some of the $R_e$'s were shortened unevenly to the values shown in the structure 5a (Fig. 1). Another interesting feature is that $E_F$ has been moved from the minority- (in the square pyramid, $R_e = 2.48$ Å) to the majority-spin (in 5a) manifold, and now, instead of being $d$-like, it is of $s$ type, but shows a similar uneven distribution of charge: there are 0.30 $s$-type and 0.05 $d$-type electrons for each of the atoms 1 and 2 of 5a (see Table I and Table 4 in PAPS[17(c)]). The reason for this behavior (the spin change in $E_F$) is that the more bonding minority-spin manifold has been moved to lower energies, due to the chemical bond formation. [When the remaining empty MO's of minority spin of 5a (see Table 4 in PAPS[17(c)]) are further occupied until the $S=0$ state is reached, and after allowing for electronic and structural relaxation, all $R_e$'s are further shortened considerably, as the levels of more bonding character of the minority-spin manifold are occupied (see below).]

The geometry optimization for the $S=9$ state of the square pyramid ($R_e$'s = 2.48 Å) converges to a square pyramid with shorter $R_e$'s (2.24 Å for the bonds in the square base and 2.32 Å for those between the apex atom and the atoms in the square) and with a total-energy change (with respect to the initial geometry) equal to $-1.08$ eV ($-0.22$ eV/atom), for the LSDA. [This optimized $S=9$ state is 0.3 eV (0.06 eV/atom) above 5a, for LSDA.]

The geometry evolution of the square pyramid ($R_e$'s = 2.48 Å), through the optimization procedure, de-

TABLE I. Total charge distribution for the $M=19$, 17, and 15 states of $Fe_5$ in the square-base pyramid, all nearest-neighbor $R_e$'s=2.48 Å. Atoms 1, 2, 3, and 4 are in the square base. The charge distribution for each of the Fermi levels is also shown.

| Site[a] | $2S+1=19$ | $2S+1=17$ | $2S+1=15$ | $2S+1=17$[b] |
|---|---|---|---|---|
| Fe(1) | 25.953 | 25.805 | 25.997 | 25.970 |
| Fe(2) | 25.953 | 25.193 | 25.997 | 26.041 |
| Fe(3) | 25.953 | 25.805 | 25.997 | 25.970 |
| Fe(4) | 25.953 | 26.193 | 25.997 | 26.041 |
| Fe(5) | 26.188 | 26.004 | 26.013 | 25.979 |
| $E_F$ | $s^{\uparrow}$[c] | $d^{\downarrow}$[c] | $d^{\downarrow}$[c] | $s^{\uparrow}$[c] |
| Fe(1) | 0.042 | 0.066 | 0.049 | 0.000 |
| Fe(2) | 0.042 | 0.322 | 0.422 | 0.303 |
| Fe(3) | 0.042 | 0.066 | 0.049 | 0.000 |
| Fe(4) | 0.042 | 0.322 | 0.413 | 0.303 |
| Fe(5) | 0.469 | 0.018 | 0.014 | 0.000 |

[a]In this order, atoms 1, 3, and 5 correspond to atoms 1, 2, and 3 of 5a (Fig. 1), respectively; similarly, sites 2 and 4 correspond to 4 and 5.
[b]For the ground state 5a.
[c]Main contributions are of this orbital type at the Fermi level.

pends on the nature of the chosen state. Indeed, in TM clusters different total-spin states give rise to different types of chemical bond, and to different patterns of charge distributions (which in turn build up different types of magnetic arrangements). This is illustrated clearly by $Fe_5$. In Table I is shown the total charge distribution for the $S=9$, 8, and 7 states of the square pyramid, and also that for the computed ground state 5a together with the charge distribution for each $E_F$. For the $S=9$ state, the total charge on the square is evenly distributed; additionally, the $s$-type $E_F$ also shows a uniform charge distribution on the square, which gives rise, during the geometry relaxation, to compensated atomic forces in the square. For the $S=8$ state, the total charge distribution as well as that of the $d$-type $E_F$ are unevenly distributed on the square, which gives rise to uneven atomic forces on the square, which produce its distortion and eventually the convergence into the distorted trigonal bipyramid 5a. The importance of the atomic forces of $d$ type is underlined by these results.

The structure 5a may be regarded as an attempt of the system to maximize the number of NNB's. The shortest $R_e$'s of 5a, 2.22 Å, match those of 4a, 2.22 Å. The trigonal bipyramid 5b is energetically quasidegenerate with 5a, for the LSDA. (In 5b the equatorial $R_e$'s are 2.36 Å for LSDA and 2.37 Å for NL, while the axial to equatorial ones are 2.21 Å in the LSDA and 2.22 Å in the NL). The NL potential breaks this degeneracy. After a NL relaxation 5b is 0.25 eV ($\simeq$6.0 kcal/mol) higher than 5a. The total spin of 5b is equal to 7, while its state with $S=8$ is 0.13 eV higher. Although the difference is small, this is the reverse order from that of 5a where the state with $S=7$ is 0.01 eV higher than the one with $S=8$.

The structure 5a may be viewed as a Jahn-Teller distortion of the $S=8$ state of 5b, which has a degenerate electronic state (there is one electron in the twofold-degenerate $s$-like MO at the top of the majority-spin manifold), and is therefore unstable. The result is the stabilization of the higher-spin state, $S=8$, in the more open structure 5a. This was the reverse for $Fe_4$ and $Fe_3$ where the stability of the compact structures was enhanced by the magnetic energy, as shown above and as pointed out previously.[23] For $Fe_5$, the magnetic energy depends critically on the chemical environment or number of NNB's.

The 2D geometry of $Fe_5$, structure 5c, is 0.25 eV/atom above 5a. It looks like a compressed pentagon with bond lengths equal to 2.08, 2.20, and 2.21 Å.

The nonmagnetic state of $Fe_5$, in the same geometry as in 5a, is located 0.95 eV/atom above the magnetic structure 5a. After a (LSDA) geometry relaxation the nonmagnetic state of $Fe_5$ is 0.74 eV/atom above 5a. It remains in a similar structure to 5a, but with substantially shortened $R_e$'s: those of 2.23, 2.22, and 2.32 Å, in 5a become 2.07, 2.09, and 2.20 Å, respectively, in the nonmagnetic structure.

### F. Clusters with bulk geometries

We have also calculated the electronic structure of $Fe_n$ ($n \leq 5$) clusters constrained to have $R_e$'s equal to the nearest-neighbor distance, 2.48 Å, in bulk iron. In fact, most of the previous theoretical studies on iron clusters have been performed under this constraint.[13,44] Below we will show that such an approximation leads to a quite different physical picture from that found for the true ground-state geometries.

For $Fe_3$ we have chosen a triangular geometry ($R_e=2.48$ Å). This cluster has a lowest-energy state of high spin, $S=6$, just the superposition of the aligned atomic spins, and $E_F$ is $s^{\uparrow}$-like. This bulk fragment is located +1.23 eV (+0.09 eV) above the ground-state geometry 3a at the LSDA (NL) level. We agree with Tatewaki, Tomonari, and Nakamura[13] in that $Fe_3$ ($R_e$'s=2.48 Å) has $S=6$. However, $E_F$ was found to be $d$-like rather than $s$-like using the ΔSCF approach.[13]

For $Fe_4$ we have chosen a tetrahedral structure ($R_e$'s=2.48 Å). Here, the lowest energy state has $S=6$, a $s^{\uparrow}$-like $E_F$, and is located +1.32 eV (+0.41 eV) above the ground-state structure 4a at the LSDA (NL) level. [We have also considered the square geometry with $R_e$'s=2.48 Å; this structure, with $S=7$ and a $d^{\uparrow}$-like $E_F$, was located 0.69 eV (LSDA) above the tetrahedron, with $R_e$'s=2.48 Å.]

For $Fe_5$ we have chosen a pyramidal square geometry ($R_e$'s=2.48 Å). This geometrical arrangement has been widely used in studies of TM-surface–ligand[46] and TM-TM interactions.[13] Here are our main results for this bulk fragment: (i) Its lowest-energy state [located +1.38 eV (+0.23 eV) above the ground-state geometry 5a at the LSDA (NL) level] is able to support an average magnetization equal to 3.6 spins/atom, $S=9$: there are 3.59 spins/atom at the square's sites and 3.65 spins/atom at the apex atom. $E_F$ is predominantly $s^{\uparrow}$-like delocalized throughout the cluster (see Table I). (ii) The magnetic state with $S=8$, 3.2 spins/atom, is only 0.057 eV above

the $S=9$ state. For $S=8$, $E_F$ is mainly $d^{\downarrow}$ type, localized principally between two opposite atoms in the square base. (iii) The state with $S=7$, 2.8 spins/atom is higher in energy, 0.79 eV above the $S=9$ state. Here $E_F$ is also $d^{\downarrow}$ type.

In summary, the lowest-energy states for $Fe_2$, $Fe_3$, $Fe_4$, and $Fe_5$, constrained to have $R_e=2.48$ Å, are located $+1.39(+0.94)$, $+1.23(+0.09)$, $+1.32(+0.41)$, and $+1.38$ eV ($+0.23$ eV), respectively, above their corresponding ground-state geometries, at the LSDA (NL) level (see Fig. 1). It is interesting to observe that whereas the LSDA gives, in all cases, a large total-energy difference (between bulk and ground-state clusters), the NL approach tends to decrease this difference as the cluster size increases.

The SCF electronic structures for the bulk iron clusters ($R_e$'s=2.48 Å) show total-spin $S$ states ($2S+1=13,13$, and 19 for $Fe_3$, $Fe_4$, and $Fe_5$, respectively), which are, in general (the exception is $Fe_4$), larger than those found for the ground-state structures (see Fig. 1). This means that at $R_e=2.48$ Å the spin-pairing process (that is, the chemical bond formation) in $Fe_n$ ($n\leq 5$) has not been switched on completely. This would lead to unrealistic estimates of properties such as binding energies and/or magnetic moments.

Finally, the ground-state geometry of $Fe_5$ (a distorted trigonal bypyramid) has a different shape and $R_e$'s from those of the bulk cluster (a square pyramid). These results show that there are substantial differences between the properties of bulk fragments and those of isolated, geometry-relaxed iron clusters.

## IV. VIBRATIONAL FREQUENCIES

In the previous section it was shown that a given $Fe_n$ cluster presents several states, of different total spin and dimensionality. Here we present vibrational analysis for the calculated ground-state structures. The harmonic approximation has been used with two-point numerical differentiation of gradients.[31] Additionally, the infrared intensities were calculated by two-point differencing of the dipole moments. Experimental data for vibrational frequencies ($\omega_e$'s) and structural parameters ($R_e$'s and bond angles) for $Fe_n$ are very scarce. Values of $R_e$ and $\omega_e$ exist for $Fe_2$ and infrared lines have been tentatively assigned to $Fe_3$. It is therefore important to establish the accuracy of the density-functional-calculated frequencies in view of their use for guiding future assignments. Furthermore, as will be seen below, the agreement with experiment is far less satisfactory than for other systems involving TM-TM bonds that have been studied with DFT[8] and, hence, they may be very useful as demanding benchmarks for the development of new methodology.

Table II contains the calculated $\omega_e$'s for $Fe_2$–$Fe_5$. It should be noted that, to our knowledge, $Fe_5$ is the largest TM cluster for which such vibrational analysis has yet been performed.

For $Fe_2$ we have estimated 497 $cm^{-1}$ (LSDA) and 474 $cm^{-1}$ (NL) for $\omega_e$. The NL $\omega_e$ is relatively close to the configuration-interaction (CI) estimation of Tomonari and Tatewaki,[41] 448.5 $cm^{-1}$. Lower than these values is the LSDA result, 418 $cm^{-1}$, of Chen *et al.*[23] These theoretical estimations show a huge discrepancy, greater than 100 $cm^{-1}$, with respect to the experimental results of Moskovits and co-workers,[47] 299.6 $cm^{-1}$, obtained by resonance Raman techniques and of Leopold and Lineberger,[49] $300\pm15$ $cm^{-1}$, obtained by negative-ion photoelectron spectroscopy. [Reported errors in $\omega_e$ calculated using various DFT techniques for dimers of other $3d$ metals[8] are smaller: 40 $cm^{-1}$ ($Sc_2$), 60 $cm^{-1}$ ($V_2$), 30 $cm^{-1}$ ($Cr_2$), 20 $cm^{-1}$ ($Mn_2$), and 20 $cm^{-1}$ ($Cu_2$)]. In TM's, particularly in iron systems, there is a delicate balance between exchange and correlation, between magnetism and chemical bonding, between populating $d$ and $s$ electrons, etc. It would seem that the current local and nonlocal functionals do not have the balance quite right and this is manifested in the large error of $\omega_e$ for $Fe_2$ (although there is no *a priori* reason that $Fe_2$ should present more difficulties than its neighbors in the periodic table).

It may be pertinent to note that the errors are similar for the DFT techniques as for the CI calculations. One would expect a difficulty in adequately correlating the $d$ electrons. As we have seen, in addition to the $4s\sigma_g$ bond, there is a large $d$ contribution to the bonding in $Fe_2$. It is interesting to observe that, under the assumption of a single $4s\sigma_g$ bond and using CI techniques,[42] the calculated $\omega_e$ for $Fe_2$ is 204 $cm^{-1}$. This theoretical value is $\simeq 100$ $cm^{-1}$ below the experimental one, and is, effectively, in the regime where the bonding is dominated by the $4s\sigma_g$ MO. For example, the experimental frequency[8] for $Cu_2$ is 266.1 $cm^{-1}$. For $Cu_2$ we have calculated[50] 216 $cm^{-1}$ for $\omega_e$ (LSDA). This estimate is in much better agreement with the experimental value than is the case for $Fe_2$. That the correlation of the $d$ and $s$ valence electrons is one of the limiting factors in the calculation of $\omega_e$ for $Fe_2$ is also reflected in the calculated values of IP and BDE for these species, which show large discrepancies with respect to the experimental results (see below).

Our vibrational analysis for the structure 3a of $Fe_3$ (Fig. 1) indicates three real frequencies 270 (3.3), 274 (3.4), and 433 $cm^{-1}$ ($<10^{-3}$ km/mol) for the LSDA, and 259 (4.2), 288 (10.6), and 470 $cm^{-1}$ (0.10 km/mol) at the NL level; the values in parentheses are the infrared intensities. The symmetric stretching mode corresponds to 274 $cm^{-1}$ (LSDA) or 288 $cm^{-1}$ (NL). The far-infrared spectrum of iron clusters in an argon matrix[45] shows two bands at 180 and 386 $cm^{-1}$, and a shoulder at about 220 $cm^{-1}$. As in $Fe_2$, the calculated $\omega$'s for $Fe_3$ are above the experimental values. Nour *et al.* have assigned 220 $cm^{-1}$ to the symmetric stretching model. If we assume that the overestimation of $\omega_e$ found for $Fe_2$ is systematic then experiment (220 $cm^{-1}$) and theory [274 $cm^{-1}$ (LSDA) or 288 $cm^{-1}$ (NL)], agree in the assignment for the symmetric stretching mode. However, Nour *et al.* have assigned the weak far-infrared band at 386 $cm^{-1}$ to some iron atom impurities. (This value has been quoted in parentheses in Table II.) Our theoretical results [433 $cm^{-1}$ (LSDA) or 470 $cm^{-1}$ (NL)] indicate that this band may belong to $Fe_3$, again assuming a systematic bias toward high frequency in the calculations. Moreover, the far-infrared spectra for $Ni_3$ shows a similar pattern: a

strong band at 198 and weaker bands at 300 and 405 $cm^{-1}$. By similar arguments as for $Fe_3$, Nour *et al.* have disregarded 405 $cm^{-1}$ as a frequency for $Ni_3$. Our results indicate that this value may in fact correspond to a vibration of $Ni_3$.

The vibrational analysis for structure 4a of $Fe_4$ produces six real frequencies: 103 (2.6), 112 (7.7), 222 (13.2), 223 (3.4), 227 (0.42), and 412 $cm^{-1}$ (3.4 km/mol). The values in parentheses are the infrared intensities. These $\omega_e$'s are in the range 103–412 $cm^{-1}$. Similarly, for the structure 5a of $Fe_5$ we have obtained nine real frequencies: 102 (1.0), 121 (4.6), 141 (0.4), 191 (1.9), 205 (0.04), 256 (4.3), 270 (0.54), 323 (1.4), and 401 $cm^{-1}$ (1.5 km/mol). Now, the $\omega_e$'s for $Fe_5$ are in the range 102–401 $cm^{-1}$. These results confirm that the structures 4a and 5a are indeed local minima on the potential energy surface. The exhibited trend is the following: in $Fe_4$ and $Fe_5$ there are vibrational modes of high frequency (as in $Fe_2$ and $Fe_3$), but also there have started to appear vibrational modes of low frequency, $\simeq 100$ $cm^{-1}$. These soft vibrational modes will converge (in the limit of a large $Fe_n$ cluster, $n \rightarrow \infty$) into the lower-frequency part of the phonon spectrum. It should be remembered that no account of anharmonicity has been taken and this is likely to be important for the low-frequency modes.

As far as we know, this is the first time that the frequencies for a TM cluster bigger than the dimer have been calculated. There are no experimental frequencies for $Fe_4$ and $Fe_5$. On the basis of experimental and calculated frequencies for $Fe_2$ and $Fe_3$ we predict that the frequencies given in Table II for $Fe_4$ and $Fe_5$ will be somewhat too high.

## V. BINDING ENERGIES

The $D_e$'s of $Fe_2$–$Fe_5$ at different levels of calculation are shown in Table II. Our results for the LSDA are close to those of Chen *et al.*[23] up to $n=4$ [the discrepancy, 0.2–0.3 eV/atom, may be due to a different configuration for the atom (it is not stated in Ref. 23 whether the experimental or the LSD ground state was chosen), or to differences in the computational details]. Compared with the experimental $D_e$ of $Fe_2$, 1.30 eV,[47] and 1.14 eV,[7] the LSDA overestimates this property by more than a factor of 3. The introduction of NL corrections improves dramatically, $\simeq 1$ eV, the estimation of

TABLE II. Molecular parameters $D_e$, $R_e$, and $\omega_e$ of $Fe_n$ ($n \leq 5$) clusters in their calculated ground states.

| | $Fe_2$ | $Fe_3$ | $Fe_4$ | $Fe_5$ |
|---|---|---|---|---|
| | | $D_e$ (eV) | | |
| LSDA[a] | 4.38 | 8.26 | 13.08 | 17.93 |
| LSDA[b] | 4.05 | 7.81 | 12.29 | |
| NL[c] | 3.24 | 5.99 | 9.83 | 13.89 |
| NL-NS[d] | 2.08 | 4.23 | 7.48 | 10.98 |
| CI[e] | −1.29 | | | |
| Expt. | 1.14[f], 1.30[g] | | | |
| | | $R_e$ (Å) | | |
| LSDA[a] | 1.96 | 2.10 | 2.22 | 2.22–2.32[h] |
| LSDA[b] | 1.98 | 2.04 | 2.25 | |
| NL | 2.00 | 2.10 | 2.22 | 2.23–2.31[h] |
| CI[e] | 2.02 | | | |
| Expt. | 1.87[i], 2.02[j] | | | |
| | | $\omega_e$ ($cm^{-1}$) | | |
| LSDA[a] | 497 | 270, 274, 433 | 103, 112, 222*i*<br>223, 227, 412 | 102, 121, 141,<br>191, 205, 256,<br>270, 323, 401 |
| LSDA[b] | 418 | | | |
| NL | 474 | | | |
| CI[e] | 448.5 | | | |
| Expt. | 299.6[k] | 180, 220, (386)[l] | | |

[a]LSDA results for the structures 2a, 3a, 4a, and 5a of Fig. 1; with respect to spherical $^5D$ Fe atoms.
[b]LSDA results from Ref. 23.
[c]NL spin-density results with respect to spherical $^5D$ Fe atoms.
[d]NL spin-density results with respect to nonspherical $^5D$ Fe atoms.
[e]CI results from Ref. 41; $D_e$ is with respect to $^5D$ Fe atoms.
[f]From Ref. 7.
[g]From Ref. 47(a).
[h]Only the range of the shortest distances is indicated (see Fig. 1).
[i]From Ref. 40.
[j]From Ref. 39.
[k]From Ref. 47(b).
[l]From Ref. 45; see text.

$D_e$. Furthermore, removal of the constraint of a spherical atomic charge density,[35] produces a deeper atomic energy if a NL SCF calculation is done, which in turn improves the estimation of $D_e$. In this way, the $D_e$ for $Fe_2$, 2.08 eV, is overestimated by about 0.7 eV. We have found[51] similar difficulties in the calculation of $D_e$ for other systems containing the Fe atom, such as the Fe-CO molecule, where our best estimate, 1.3 eV (with the NL nonspherical approach), differs by about 0.8 eV from the experimental values; see Ref. 51 for more details.

The estimate of $D_e$ for $Fe_2$, as mentioned above, has been made using an auxiliary basis set to fit the XC potential and evaluate the XC energy. Better results may be obtained by evaluation of the XC terms numerically through the use of an EXTRAFINE (see Ref. 31) grid which, for $Fe_2$, consists of 2745 points for each atom. In this way the NL functional of Perdew and Wang[26,27] proposed in 1986 (PW86), produces 3.13 eV (with respect to spherical Fe atoms) and 1.70 eV (with respect to nonspherical Fe atoms) for the $D_e$ of $Fe_2$. (The corresponding NL fitting values are 3.23 and 2.08 eV, respectively). So, the numerical evaluation of the XC terms, though much more demanding computationally, results in an improvement over the fitting procedure, particularly at the NL nonspherical level. However, they still differ by about 0.5 eV from the experimental results 1.14 (Ref. 7) and 1.30 eV.[47] Using this numerical procedure, the implementation in our code of the NL functional proposed recently by Perdew and co-workers[48] produces 3.5 eV (with respect to spherical atoms) and 1.94 eV (with respect to nonspherical Fe atoms) for the $D_e$ of $Fe_2$. The PW86 $D_e$'s for $Fe_2$ are in better agreement with the experimental results than those obtained by means of the functional of Ref. 48. Similarly, the PW86 functional yields 5.87 eV (with respect to spherical Fe atoms) and 3.73 eV (with respect to nonspherical atoms) for the $D_e$ of $Fe_3$. These results should be compared with those obtained by means of the functional of Ref. 48, 6.65 eV (spherical) and 4.25 eV (nonspherical). PW86 produces an equilateral triangle, with $R_e = 2.10$ Å, for the ground state of $Fe_3$. The functional of Ref. 48 gives the same structure with $R_e = 2.11$ Å. The difference in $R_e$'s is relatively small. So, concerning the binding energies, the older functional of Perdew and Wang[26,27] does a better job in the present context, than the new one of Perdew and coworkers.[48] In what follows, we will continue our discussion with results obtained by means of the NL functional proposed in 1986.

The nonspherical NL treatment of the atom is the best one can currently do within DFT. Higher accuracy will require a better understanding of open-shell multiplets in terms of DFT, aside from the improvement of the nonlocality in the functional, in order to account properly for the exchange-correlation interactions in this kind of system.

## VI. IONIZATION POTENTIALS

The calculated NL adiabatic IP's for the $Fe_n$ ($n \leq 5$) ground-state structures are shown in Table III, together with the experimental[5] and the symmetry-broken ΔSCF *ab initio* results for bulk fragments.[13] The structural relaxations were +0.09, +0.05, and −0.002 Å for $Fe_2^+$, $Fe_3^+$, and $Fe_4^+$, respectively (see Fig. 2). This means that for $Fe_2$ the $1\delta_{E_F}{}^{\downarrow}$ MO (from which the electron was ionized) is not as weakly bonding as expected; it behaves as a bonding orbital whereas in $Fe_3$ and $Fe_4$ the electrons at $E_F$ behave as weakly bonding or as nonbonding. In $Fe_3$ a $d^{\downarrow}$ electron was ionized while in $Fe_4$ a delocalized $s^{\uparrow}$ electron was removed. In $Fe_5^+$ the relaxations range from +0.002 to +0.076 Å except for one of −0.116 Å, between sites 1 and 2 of 5a. Here, an $s^{\uparrow}$ electron was ionized, mainly localized between these sites. The change in

TABLE III. LSDA and NL ionization potentials (eV) of $Fe_n$ ($n \leq 5$) clusters, calculated for the ground states, for some isomers, and for some bulk fragments.

| Cluster | Structure | LSDA | NL | ΔSCF[a] | Expt.[b] |
|---|---|---|---|---|---|
| Fe | | 8.10 | 8.16[c] | | 7.9 |
| $Fe_2$ | 2a[d] | 7.21 | 7.00[c] | 5.3 | 6.3 |
| $Fe_3$ | 3a[d] | 6.27 | 6.20[c] | | 6.4–6.5 |
| $Fe_4$ | 4a[d] | 5.90 | 6.20[c] | | 6.3–6.5 |
| $Fe_4$ | 4b[d] | 6.16 | 6.34 | | |
| $Fe_5$ | 5a[d] | 6.37 | 6.52[c] | | 5.9–6.0 |
| $Fe_5$ | 5b[d] | 6.36 | | | |
| $Fe_5$ | 5c[d] | 6.59 | | | |
| $Fe_3$ | trigonal[e] | 6.22 | 6.66 | 5.9 | |
| $Fe_4$ | square[e] | 6.55 | 6.64 | 5.9 | |
| $Fe_4$ | tetrahedral[e] | 5.90 | 6.26 | | |
| $Fe_5$ | square pyramid[e] | 6.25 | 6.34 | 6.4 | |

[a]ΔSCF *ab initio* results from Ref. 13.
[b]From Ref. 5.
[c]Adiabatic IP's for the ground states, as indicated in Fig. 2 of Ref. 24.
[d]From this structure (see Fig. 1) was calculated the geometry and electronic-structure relaxation for the cation.
[e]Bulk fragments with fixed bond lengths equal to 2.48 Å.

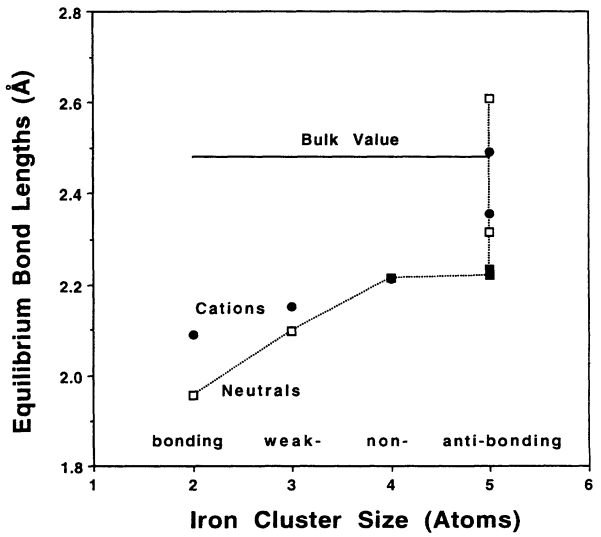


FIG. 2. Equilibrium bond lengths for the calculated ground-state structures of $Fe_n$ ($n \leq 5$). Open squares represent neutrals and solid circles cations. The bonding character of the Fermi level is labeled.

$R_{12}$ indicates an antibonding behavior of $E_F$ in $Fe_5$. Our IP values mimic the experimental pattern and are nearer to this than are the ΔSCF ones. The biggest discrepancy is for $Fe_2$, where the NL IP is $\simeq 0.7$ eV higher, while the ΔSCF one is $\simeq 1$ eV lower. For $Fe_5$, DFT and ΔSCF yield overestimates, by 0.57 and by 0.45 eV. For $n=3$ and 4, our agreement with experiment is excellent. The ΔSCF calculations[13] revealed *d*-like $E_F$'s for $n=2-5$. We have found $E_F$'s of *d* type for $n=2$ and 3 and of *s* type for $n=4$ and 5. The changes in the electronic structure, from the unoptimized to the fully relaxed (structural and electronic) geometries, with the most noticeable ones in the compositions of the Fermi levels, stress the importance of geometry optimization for iron cluster properties. Even in this small range, $n \leq 5$, theory and experiment show an overall decrease of the IP's, as needed to converge toward the bulk work function.

In the previous section, we showed the dramatic improvement of the calculated $D_e$'s produced by the NL corrections. In Table III are shown the LSDA and NL adiabatic IP's calculated for the ground states of the $Fe_n$ ($n \leq 5$) clusters, along with the IP's for some isomers, and for some *bulk* fragments (i.e., those calculated for unoptimized geometries, with fixed bond lengths equal to 2.48 Å). We will discuss the LSDA and NL IP's for the ground states. For Fe and $Fe_3$ there are slight differences between LSDA and NL IP's. For $Fe_2$ and $Fe_4$ the NL corrections clearly improve the IP's, by 0.2–0.3 eV, with respect to those at the LSDA level. However, for $Fe_5$ the LSDA is nearer to experiment than NL (albeit by only 0.15 eV) (see Table III). In other words, the screening properties of the NL functional are not demonstrably superior to those of the LSDA. Even with the $X\alpha$ functional, reasonable IP's have been obtained for some iron clusters. For instance, using the SCF $X\alpha$ SW method,[5] and through a transition-state calculation, the vertical IP for $Fe_3$, 6.30 eV, is remarkably close to the experimental value, 6.4–6.5 eV. In the vertical approach, our calculated IP's for $Fe_3$ are 6.35 and 6.34 eV for the LSDA and NL (as shown, the structural relaxation makes these values deviate slightly from the experimental one, see Table III). So, the LSDA should be an adequate level of theory for the computation and analysis of IP's in this kind of system. However, as shown in the previous section for the $D_e$'s, an accurate analysis of the binding properties of iron clusters requires NL functionals. For this reason we have performed a careful analysis of the IP's at the NL level, as shown in Table III, where this level of theory is confronted with experimental and theoretical results. This information is useful for the study of BDE's of $Fe_n^+$. Indeed, we have shown in Ref. 24 that, at the NL level of theory, the calculated BDE's for $Fe_n$ and $Fe_n^+$ ($n \leq 5$), reproduce the main trends that have been determined experimentally[7] for this property.

## VII. ELECTRON AFFINITIES

We have also considered the process of attaching one extra electron to the ground states of $Fe_n$ ($n \leq 5$). After a full relaxation our main results for $Fe_2^-$ are the following. (1) In the lowest-energy state the extra electron goes into the $4s\sigma_u^{\uparrow}$ MO, as predicted by Leopold and Lineberger.[49] This results in a molecular state of the type $^8\Delta_g$ ($=^7\Delta_u + 4s\sigma_u$); effectively this state was also found by Tomonari and Tatewaki.[41] However, the *ab initio* $4\sigma_u$ is *p*-like, predominantly; whereas in our results although there is a substantial *p* contribution, $4\sigma_u$ is predominantly 4*s*-like, as was originally predicted.[49] (2) the LSDA and NL $R_e$ for $Fe_2^-$ is 2.07 Å, in both cases; the elongation with respect to $Fe_2$, of 0.05 Å, confirms the prediction of $0.08 \pm 0.02$ Å made on experimental grounds.[49] The CI result,[41] of 0.03 Å, is also of the right order of magnitude. (3) $Fe_2^-$ has a lower energy than $Fe_2$, 0.95 eV for the LSDA and 1.31 eV for NL, so that our computed adiabatic electron affinity (EA) is in reasonable accord with the experimental value, 0.90 eV.[49] The CI estimation is 0.45 eV.[41] (4) The calculated frequencies for $Fe_2^-$, 412 $cm^{-1}$ (LSDA) and 345 $cm^{-1}$ (NL), give ratios $\omega_e(Fe_2)/\omega_e(Fe_2^-)$, of 0.83 and 0.73; close to experimental and *ab initio* ratios, 0.83.[49,41] Note that the NL $\omega_e$ for $Fe_2^-$ is closer to the experimental value,[49] $250 \pm 20$ $cm^{-1}$, than that determined with the LSDA. However, the LSDA does a somewhat better job than the NL functional for both the EA and the $\omega$ ratios.

Here are our main results for $Fe_3^-$. It remains in a structure like 3a (see Fig. 1), but with longer, +0.08 Å, bond lengths. [The linear structure of $Fe_3^-$ is located $\simeq 1.5$ eV (LSDA) above the trigonal one.] Within the LSDA $Fe_3^-$ is 1.37 eV more stable than $Fe_3$, while for NL it is 2.0 eV more stable. Our computed BDE for $Fe_3^-$ is 2.86 eV (NL); the suggested experimental value is 1.9 eV, deduced under the assumption of similar bonding schemes for charged (positive and negative) and neutral trimers.[6] In this triad ($Fe_3^-$, $Fe_3^+$, and $Fe_3$), theory and experiment agree that $Fe_3^-$ has the largest BDE. See Ref. 24 for more details of the calculations of BDE's. (Here we have used the relation $Fe_3^- \rightarrow Fe_2^- + Fe$, and performed NL calculations for $Fe_3^-$, $Fe_2^-$, and for nonspherical Fe.)

In the ground state of $Fe_4$ the added electron is distributed throughout the cluster by the highly delocalized *s*-type $E_F$ MO (this is a threefold-degenerate MO) (see Table 3 in PAPS[17(c)]). Our vertical (keeping the same geometry as in 4a) EA is 1.67 eV. After structural relaxation, the adiabatic EA of $Fe_4$ is 1.69 eV. In fact, the $R_e$'s in $Fe_4^-$ have been increased slightly, by less than 0.01 Å, with respect to those of $Fe_4$. These EA's are for the LSDA. The vertical NL EA of $Fe_4$ is 2.11 eV, and the adiabatic one is 2.19 eV.

The added electron to the ground state of $Fe_5$ goes into the lowest unoccupied MO of minority spin ($\epsilon_i = 4.11$ eV, see Table 4 in PAPS[17(c)]), which results in a molecular state with $M = 2S+1 = 18$ for $Fe_5^-$, with a vertical EA equal to 2.04 eV, for the LSDA. (The $M=16$ state of $Fe_5^-$ is 0.34 eV above the $M=18$ state.) In contrast to $Fe_5^+$, the structural relaxation in $Fe_5^-$ is very small; its $R_e$'s have been increased by about 0.02 Å with respect to those of $Fe_5$. The adiabatic LSDA EA of $Fe_5$, 2.08 eV, is essentially the same as the vertical one. The vertical NL EA of $Fe_5$ is equal to 2.28 eV; a similar value is expected for the adiabatic one. To summarize this section: the

EA's of $Fe_n$ increase with increasing cluster size, from (LSDA values) 0.90 (for $Fe_2$) to 2.08 eV (for $Fe_5$).

## VIII. CONCLUSIONS

In conclusion, recently developed techniques, as exemplified by the Gaussian DFT code deMon have allowed an unprecedented level of analysis of the properties of small transition-metal clusters. The main features of the experimental trends ($R_e$'s, $\omega_e$'s, $D_e$'s, $\mu$'s, IP's, BDE's, and EA's), have been accounted for and insight has been achieved as to how the structural, electronic, and magnetic parameters are involved in the stability of these clusters. The two forces, chemical and magnetic, drive the iron clusters toward ferromagnetic ground states with a maximization in chemical bond formation.

These calculations show the importance of a full optimization (geometry and electronic structure) and of the exchange-correlation effects on an accurate analysis of transition-metal cluster properties. It has been found that compact structures of $Fe_n$ ($n=2-5$) are more stable than the geometrical fragments of the iron bcc lattice. The computed ground states show equilibrium bond distances substantially shorter than the shortest distance in the crystal, 2.48 Å; although on the pentamer some bond lengths approach the bulk value. This is most transparent for the cation $Fe_5^+$, which more closely resembles (from the structural point of view) a fragment of the bulk (see Fig. 2).

For the ground states we obtained SCF high-spin-polarized electronic structures, with magnetic moments per atom enhanced over the bulk value, by 22–45%. The magnetic effects play an important role on the structural and binding properties. The nonmagnetic states are higher in energy; they remain in similar structures as the ground states but with substantially shorter $R_e$'s.

The maximization of the number of nearest-neighbor bonds and the gain in magnetic energy drives the iron clusters toward compact high-dimensional geometries. However, for the pentamer, the magnetic energy favors the more open structure 5a.

The Mulliken analyses for the computed ground states of $Fe_n$ ($n \leq 5$), revealed $d$-like Fermi levels for $n=2$ and 3, and $s$-like for $n=4$ and 5. Starting from highly localized multiple $d$ bonds on earlier clusters, the chemical bond evolves toward a delocalized $s$ pattern. The importance of the $s$-type electrons increases with increasing cluster size. (This accounts for the small difference of BDE's for neutrals and cations in the $n>5$ size range, as found experimentally.)

Our results anticipate that the anions $Fe_n^-$ would occur in very similar structures to those for neutral $Fe_n$. The structural relaxations were about +0.05, +0.08, +0.01, and +0.02 Å, for $Fe_2^-$, $Fe_3^-$, $Fe_4^-$, and $Fe_5^-$, respectively. It would be interesting to see, for instance, the results of negative-ion photoelectron spectroscopy for this kind of system. The structural relaxations for the cations (+0.09, +0.05, and −0.002 for $Fe_2^+$, $Fe_3^+$, and $Fe_4^+$, and +0.002–−0.116 Å for $Fe_5^+$) are, in general, larger than those for the anion $Fe_n^-$; however, they also remain in similar geometries as those of the ground states. Cations and anions of $Fe_2$ and $Fe_3$ show the biggest changes in $R_e$'s; these species display similar bonding schemes,[5] mainly of $d$ type. The small changes in $R_e$'s; for the cations and anions of $Fe_4$ and $Fe_5$ may be traced to the occurrence of weak "metallic" bonding at the Fermi level.

The introduction of NL gradient-type corrections shows a dramatic improvement in the estimation of the binding properties, $D_e$'s and BDE's. But even at this level of theory there remains an overestimation in the computed values, with respect to the experimental results. These properties involve the energy of the open-shell multiplets of the isolated iron atom, and this has proved to be difficult to calculate with very high accuracy within Kohn-Sham DFT in its present state. On the other hand, the calculated NL ionization potentials and electron affinities are of similar quality to those calculated with the LSDA. The local and nonlocal functionals used in this work exhibit similar screening properties.

These computations, though demanding, have all been done on general-use Silicon Graphics 4D/280 and FPS 511 servers. Extensions to fully optimized TM clusters in the 10–15-atom size range should be feasible with more powerful computing equipment. We find this prospect very exciting. Among other things, it will open up possibilities for the study of far more interesting models for reactions involving TM's than has heretofore been possible.

## ACKNOWLEDGMENTS

Valuable discussions with Leif Goodwin, Nathalie Godbout, Suzanne Sirois, Vladimir Malkin, Olga Malkina, Andreas Koster, and Mark Casida, are gratefully acknowledged. Support from NSERC and the Canadian Network of Centres of Excellence in Molecular and Interfacial Dynamics is gratefully acknowledged, as is the provision of computing resources by the Services Informatiques de l'Université de Montréal. M.C. acknowledges partial financial support from Dirección General de Asuntos del Personal Académico, Universidad Nacional Autónoma de México.

*Permanent address: Sección de Química Téorica, Facultad de Química, Universidad Nacional Autónoma de México, Delegación Coyoacán, 04510 México, Distrito Federal, Mexico.

[1]W. A. de Heer, P. Milani, and A. Châtelain, Phys. Rev. Lett. **65**, 488 (1990).

[2]J. P. Bucher, D. C. Douglas, and L. A. Bloomfield, Phys. Rev. Lett. **66**, 3052 (1991).

[3]D. M. Cox, D. J. Trevor, R. L. Whetten, E. A. Rohlfing, and A. Kaldor, Phys. Rev. B **32**, 7290 (1985).

[4]S. N. Khanna and S. Linderoth, Phys. Rev. Lett. **67**, 742 (1991).

[5]E. A. Rohlfing, D. M. Cox, A. Kaldor, and K. H. Johnson, J. Chem. Phys. **81**, 3846 (1984).
[6]S. K. Loh, D. A. Hales, L. Lian, and P. B. Armentrout, J. Chem. Phys. **90**, 5466 (1989).
[7]L. Lian, C.-X. Su, and P. B. Armentrout, J. Chem. Phys. **97**, 4072 (1992).
[8]D. R. Salahub, Adv. Chem. Phys. **69**, 447 (1987), and references therein.
[9]J. L. Martins, J. Buttet, and R. Car, Phys. Rev. B **31**, 1804 (1985).
[10]K. Raghavachari and C. M. Rohlfing, J. Chem. Phys. **89**, 2219 (1988).
[11]R. Fournier, S. B. Sinnott, and A. E. DePristo, J. Chem. Phys. **97**, 4149 (1992); **98**, 9222(E) (1993).
[12]*Metal-Ligand Interactions: From Atoms, to Clusters, to Surfaces,* Vol. 378 of *NATO Advanced Study Institute, Series C: Mathematical and Physical Sciences,* edited by D. R. Salahub and N. Russo (Kluwer, Dordrecht, 1992).
[13]H. Tatewaki, M. Tomonari, and T. Nakamura, J. Chem. Phys. **88**, 6419 (1989).
[14]C. Satoko, Chem. Phys. Lett. **83**, 111 (1981); Phys. Rev. B **30**, 1754 (1984); F. W. Averill and G. S. Painter, *ibid.* **32**, 2141 (1985); **34**, 2088 (1986).
[15]L. Versluis and T. Ziegler, J. Chem. Phys. **88**, 322 (1988).
[16]R. Fournier, J. Andzelm, and D. R. Salahub, J. Chem. Phys. **90**, 6371 (1989).
[17](a) A. St-Amant and D. R. Salahub, Chem. Phys. Lett. **169**, 387 (1990); (b) D. R. Salahub, R. Fournier, P. Mlynarski, I. Papai, A. St.-Amant, and J. Ushio, in *Density Functional Methods in Chemistry,* edited by J. Labanowski and J. Andzelm (Springer, New York, 1991); (c) See AIP document no. PAPS PRBMD-49-11842-4 for 4 pages of the Mulliken population analyses for the ground states of $Fe_n$, $n \leq 5$. Order by PAPS number and journal reference from American Institute of Physics, Physics Auxiliary Publication Service, 500 Sunnyside Boulevard, Woodbury, New York 11797-2999. The price is $1.50 for each microfiche (60 pages) or $5.00 for photocopies of up to 30 pages, and $0.15 for each additional page over 30 pages. Airmail additional. Make checks payable to the American Institute of Phyics.
[18]F. Sim, D. R. Salahub, S. Chin, and M. Dupuis, J. Chem. Phys. **95**, 4317 (1991).
[19]E. Broclawick and D. R. Salahub, Int. J. Quantum Chem. Symp. **26**, 393 (1992).
[20]L. Fan and T. Ziegler, J. Chem. Phys. **95**, 7401 (1991).
[21]L. Goodwin and D. R. Salahub, Phys. Rev. A **47**, 774 (1993).
[22]A. Goursot, I. Papai, and D. R. Salahub, J. Am. Chem. Soc. **114**, 7452 (1992).
[23]J. L. Chen, C. S. Wang, K. A. Jackson, and M. A. Pederson, Phys. Rev. B **44**, 6558 (1991).
[24]M. Castro and D. R. Salahub, Phys. Rev. B **47**, 10 955 (1993).
[25]S. H. Vosko, L. Wilk, and M. Nusair, Can. J. Phys. **58**, 1200 (1980).
[26]J. P. Perdew and Y. Wang, Phys. Rev. B **33**, 8800 (1986).
[27]J. P. Perdew, Phys. Rev. B **33**, 8822 (1986); **34**, 7406(E) (1986).
[28]A. St.-Amant, Ph.D. thesis, Université de Montréal, 1992.
[29]J. Andzelm, E. Radzio, and D. R. Salahub, J. Comput. Chem. **6**, 520 (1985).
[30]N. Godbout, D. R. Salahub, J. Andzelm, and E. Wimmer, Can. J. Chem. **70**, 560 (1992).
[31]deMon User's Guide, version 1.0 beta (Biosym Technologies, San Diego, 1992).
[32]A. D. Becke, J. Chem. Phys. **88**, 2547 (1988). The radial grid in deMon was inspired by this paper, differing only in the fact that it uses the Gaussian-Legendre quadrature scheme instead of Gauss-Chebyshev.
[33]See H. B. Schlegel, in *Ab Initio Methods in Quantum Chemistry-I,* edited by K. P. Lawley (Wiley, New York, 1987).
[34]C. E. Moore, *Atomic Energy Levels,* Natl. Bur. Stand. (U.S.) Circ. No. 467 (U.S. GPO, Washington, DC, 1949).
[35]F. W. Kutzler and G. S. Painter, Phys. Rev. Lett. **59**, 1285 (1987).
[36]C. W. Bauschlicher, Jr., J. Chem. Phys. **86**, 5591 (1987).
[37]M. W. Chase, Jr., C. A. Davies, J. R. Downey, Jr., D. J. Frurip, R. A. McDonald, and A. N. Syverud, J. Phys. Chem. Ref. Data **14**, 1179 (1985).
[38]L. A. Bloomfield *et al.* (private communication) and (unpublished).
[39]H. Purdum, P. A. Montano, G. K. Shenoy, and T. Morrison, Phys. Rev. B **25**, 4412 (1982).
[40]P. A. Montano and G. K. Shenoy, Solid State Commun. **35**, 53 (1980).
[41]M. Tomonari and H. Tatewaki, J. Chem. Phys. **88**, 1828 (1988).
[42]I. Shim and K. A. Gingerich, J. Chem. Phys. **77**, 2490 (1982).
[43]J. Callaway and C. S. Wang, Phys. Rev. B **16**, 2095 (10 977); C. S. Wang and J. Callaway, *ibid.* **15**, 298 (1977).
[44]C. Y. Yang, K. H. Johnson, D. R. Salahub, J. Kaspar, and R. P. Messmer, Phys. Rev. B **24**, 5673 (1981).
[45]E. M. Nour, C. Alfaro-Franco, K. A. Gingerich, and J. Lanne, J. Chem. Phys. **86**, 4779 (1987).
[46]P. Mlynarski and D. R. Salahub, J. Chem. Phys. **95**, 6050 (1991).
[47](a) M. Moskovits, D. P. DiLella, and W. Limm, J. Chem. Phys. **80**, 626 (1984); (b) M. Moskovits and D. P. DiLella, *ibid.* **73**, 4917 (1980).
[48]J. Perdew, Physica B **172**, 1 (1991); J. P. Perdew, J. A. Chevary, S. H. Vosko, K. A. Jackson, M. R. Pederson, D. J. Singh, and C. Fiolhais, Phys. Rev. B **46**, 6671 (1992).
[49]D. G. Leopold and W. C. Lineberger, J. Chem. Phys. **85**, 51 (1986).
[50]P. Calaminici, M. Castro, and D. R. Salahub (unpublished).
[51]M. Castro, R. Fournier, and D. R. Salahub, J. Chem. Phys. (to be published).

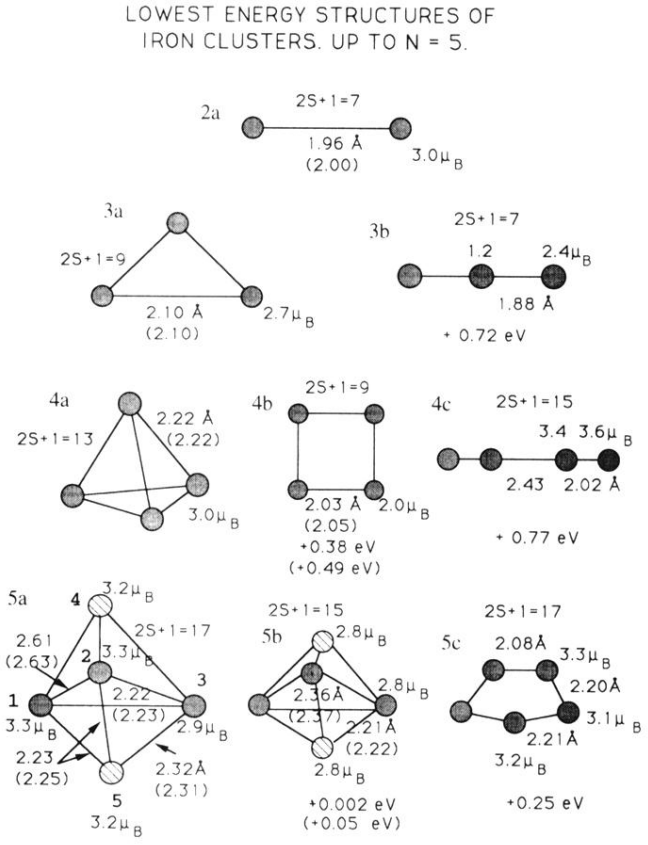


**FIG. 1.** Lowest-energy structures of $Fe_n$ ($n \leq 5$). Ground states are 2a, 3a, 4a, and 5a for $n=2$, 3, 4, and 5, respectively. Also indicated are the LSDA and NL (values in parentheses) relative energies of the isomers (in eV/atom), the multiplicity $2S+1$, the spin per atom (in bohr magnetons), and the LSDA and NL (values in parentheses) equilibrium bond lengths.